Supporting Information for ”Conformational Selection vs. Induced Fit: Insights into the Binding Mechanisms of p38α MAP Kinase Inhibitors”

Patrick Roser, Jörn Weisner, Juliane Stehle, Daniel Rauh* and Malte Drescher*

Table of Contents

Expression, purification and spin labeling of p38α

N-terminally His_6-tagged p38α constructs containing a PreScission Protease cleavage site and the mutations required for double-labeling, i.e., C119S/C162S/F327L/A172C as well as S119C, S251C, A277C, A309C, and S347C, respectively, were generated via site-directed mutagenesis and cloned into a pOPINF vector. Human p38α MAPK mutant constructs were subsequently transformed into chemically competent BL21 (DE3) E. coli, expressed and purified as described previously.[1-2] Briefly, overexpression was performed at 18 °C overnight (20 hours) while shaking at 160 rpm. Afterwards, the target proteins were purified by Ni-affinity, anion exchange, and size exclusion chromatography. The His6-tag was removed by addition of PreScission Protease prior to anion exchange chromatography. Finally, purified proteins were concentrated to approximately 20 mg/mL, snap frozen in liquid nitrogen and stored at -80 °C until further use.

To a 50 µM solution of p38α in labeling buffer (20 mM Tris, 200 mM NaCl, 5% v/v glycerol, pH 7.4) six equivalents of (1-oxyl-2,2,5,5-tetramethylpyrroline-3-methyl) methanethiosulfonate (SCBT, 25 mM in DMSO) were added and incubated overnight at 4 °C while shaking gently. The crude product was isolated using Vivaspin 4 centrifugal filters (10 kDa MWCO, Sartorius) for 6-8 times at 4 °C until no free spin label could be detected using CW EPR spectroscopy. The residue was collected in buffer to yield a final con-centration of approx. 300 µM and stored at -80 °C.

Inhibition assay

p38α at a concentration of 50-100 µM was mixed with six molar equivalents of the inhibitors RL45, RL48, Sorafenib, Regorafenib, Skepinone-L, SKF-86002, and SB203580 (10 mM in DMSO stock solutions). The mixture was incubated for 90 min at 21 °C while gently shaking the flask. The final amount of DMSO in the samples did not exceed 5% in any measurement.

Pulsed EPR Experiments

Pulsed experiments were performed either on a Bruker Elexsys E580 Q-band spectrometer using a Bruker EN 5107D2 resonator equipped with a 15 W solid state microwave amplifier and a helium gas flow system (CF935, Oxford Instruments) or a QT-II resonator equipped with a 150 W TWT and a cryogen-free system. The sample volume was 10 µL for the EN 5107D2 resonator and 60 µL for the QT- II resonator. Samples were snap frozen in liquid nitrogen and inserted into the resonator. The temperature was fixed to 50 K.

Distance measurements were carried out using a two dimensional 4-pulse DEER experiment.[3] The shot repetition time was optimized to prevent saturation of longitudinal relaxation of the nitroxide labels. Pump and observer frequencies were optimized for every sample and range between 20 and 32 ns for the pump and 22 to 46 ns for the observer pulses. The magnetic field was set to the maximum of the nitroxide spectrum and the observer pulse frequency was set to 50.4 MHz lower than the pump pulse frequency. Nuclear modulation averaging was used to suppress nuclear modulation artefacts. Accumulation times largely depended on the resonator used and the sample quality and typically ranged between 4 to 20 hours. The dipolar evolution time was optimized for each sample to yield reliable distance information while retaining a high signal-to-noise ratio.

DEER distance distribution analysis

The two dimensional raw DEER data was phase corrected for every slice, averaged and then further processed using Matlab 2017a and DeerAnalysis2016.[4] The zero time and the background start was determined using the built-in optimization function, the end of the DEER curve was cut manually to remove artefacts in the trace. The distance distribution was extracted using a three-dimensional background and Tikhonov-regularization. While the α parameter was typically determined

automatically using the L curve criterion, in some cases a slightly larger α parameter was chosen to prevent over sharpening of the distance distribution. Tikhonov validation was conducted by changing the start of the background correction region gradually from 1000 to 2500 ns while adding an additional white noise level of 1.5 times the experimental noise, resulting in 40 trials for every measurement.

Multilateration

3D modelling of the spin label distribution was carried out using the MMM 2017.2 package.[5] The distance constraints from the preceding analysis were approximated using a single Gaussian distribution profile and the parameters used as an input file for MMM. The crystal structures mentioned in the text were specifically chosen to include coordinates for the label position 172 and thus allow for a label position prediction. Each multilateration was carried out using five different distances to improve the reliability of the probability volume. For the visualization, a probability volume showing 50 percent of the total probability was chosen as supposed by MMM.

Crystal structure alignment

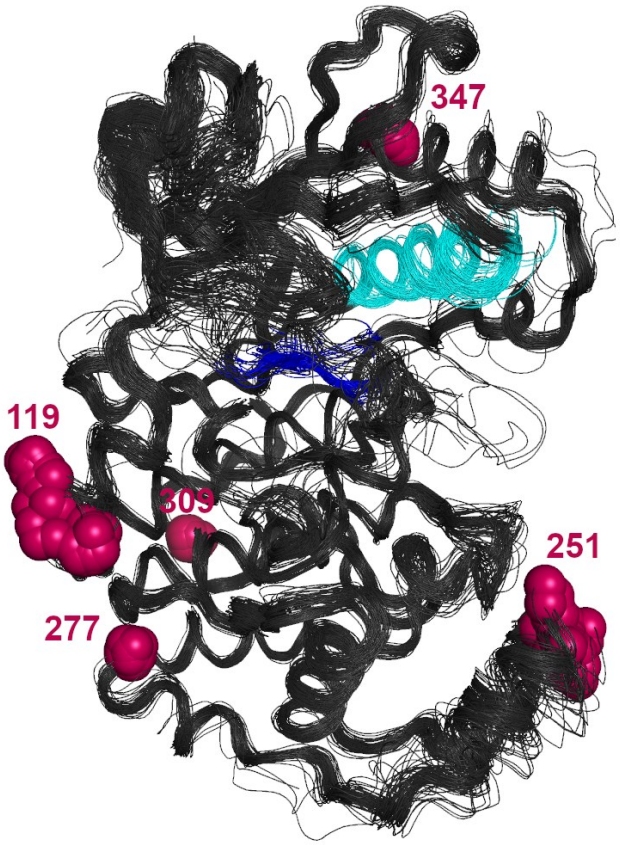

Figure S. 1: Alignment of 239 p38α (uniprot ID: Q16539) crystal structures available in the protein data bank. The protein backbones are displayed as darkgrey loops and the C-alpha atoms of secondary labeling sites at positions 119, 251, 277, 309, and 347 are depicted as pink spheres. The αC-helix and the DFG-motif are colored in cyan and blue, respectively, for better orientation. Created using PyMOL.[6]

DEER Distance data

Raw data traces for apo p38α

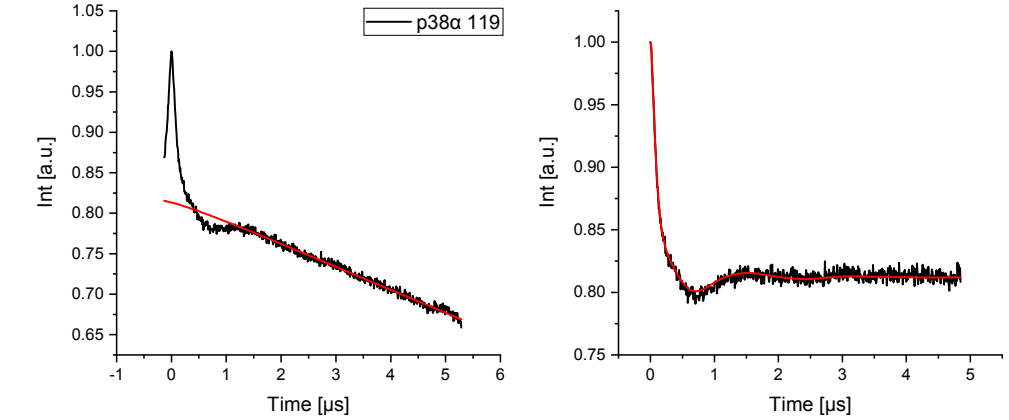

Figure S. 2: Left: Raw DEER data trace obtained for p38α 119 (black) and the corresponding background fit (red). Right: Form factor (black) and the fit obtained by Tikhonov regularization (red).

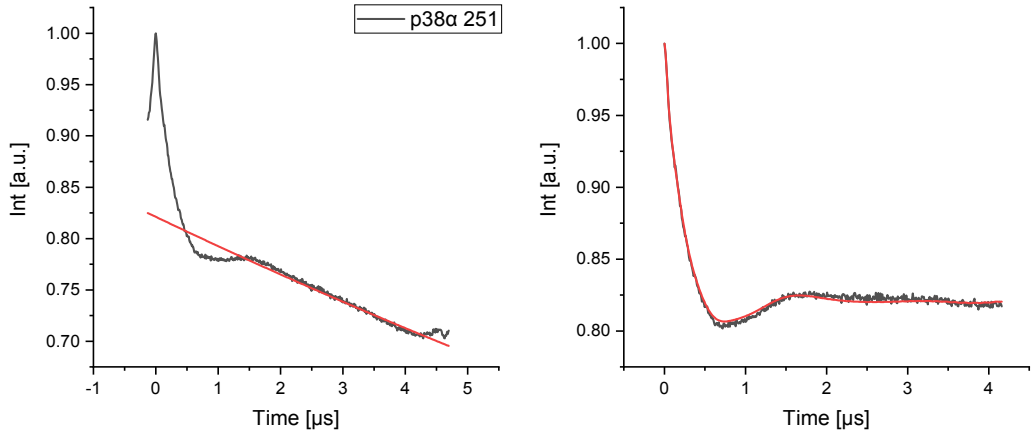

Figure S. 3: Left: Raw DEER data trace obtained for p38α 251 (black) and the corresponding background fit (red). Right: Form factor (black) and the fit obtained by Tikhonov regularization (red).

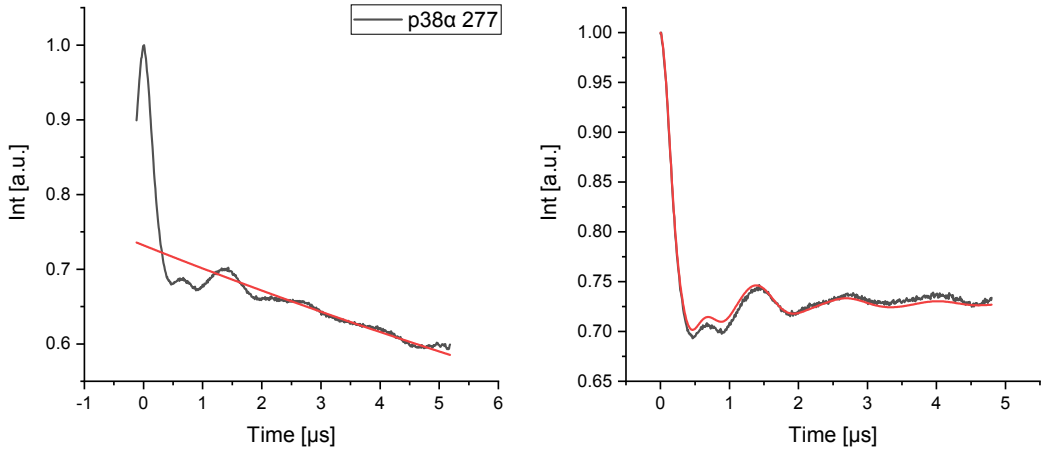

Figure S. 4: Left: Raw DEER data trace obtained for p38α 277 (black) and the corresponding background fit (red). Right: Form factor (black) and the fit obtained by Tikhonov regularization (red).

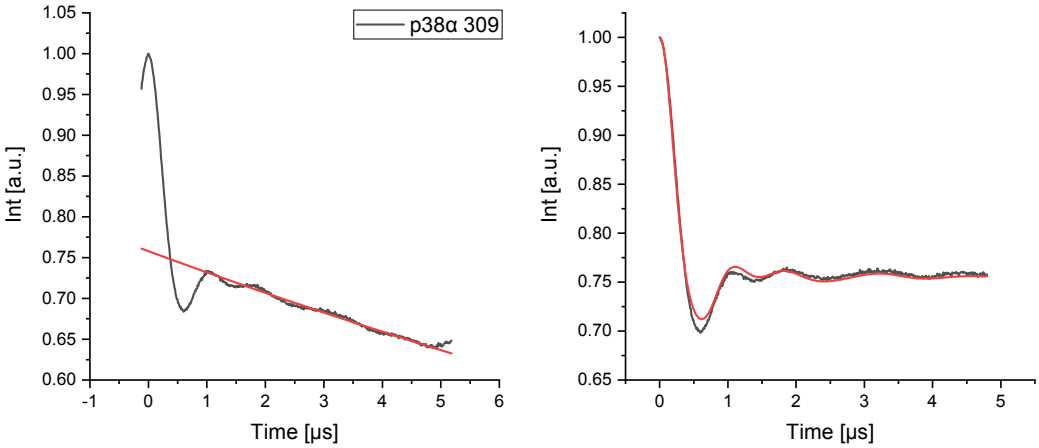

Figure S. 5: Left: Raw DEER data trace obtained for p38α 309 (black) and the corresponding background fit (red). Right: Form factor (black) and the fit obtained by Tikhonov regularization (red).

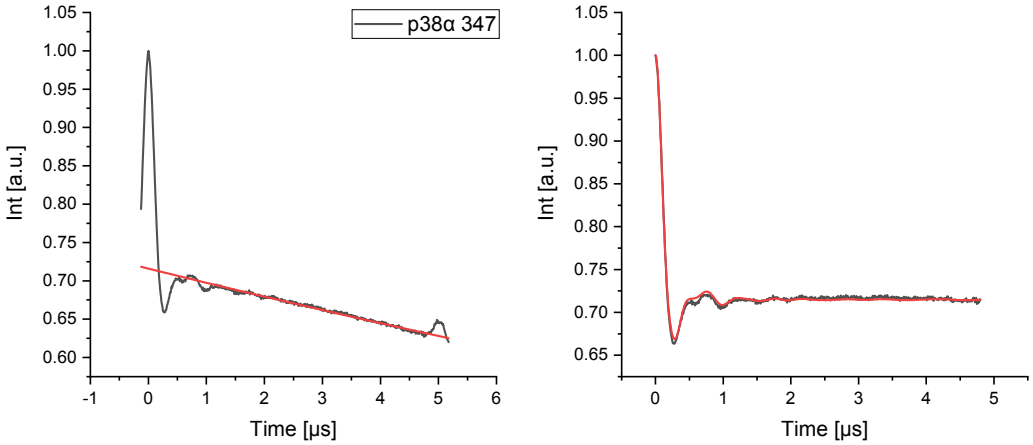

Figure S. 6: Left: Raw DEER data trace obtained for p38α 347 (black) and the corresponding background fit (red). Right: Form factor (black) and the fit obtained by Tikhonov regularization (red).

Raw data traces in presence of inhibitors

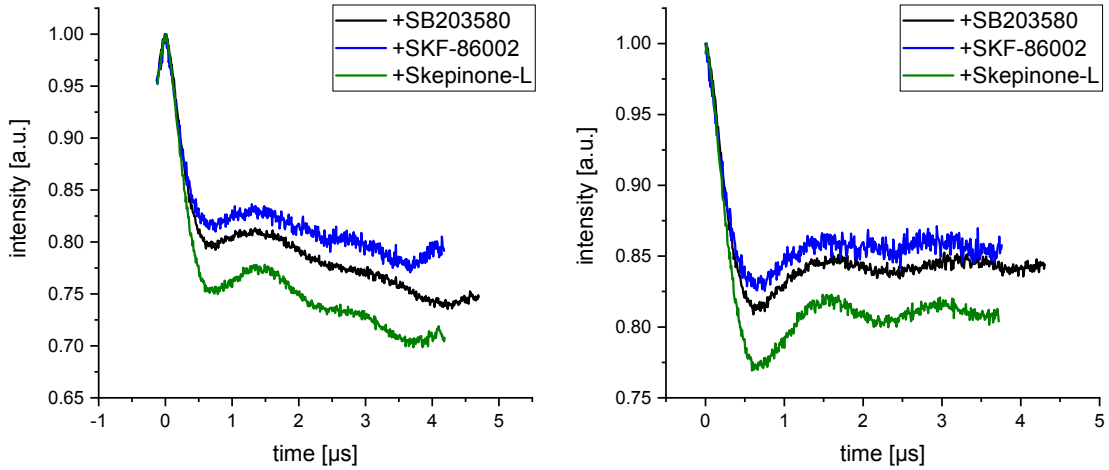

Figure S. 7: Inhibitor measurements with p38α 119. Left: Raw DEER data traces obtained for p38α 119 with the three type I inhibitors. Right: Form factors obtained for the DEER traces.

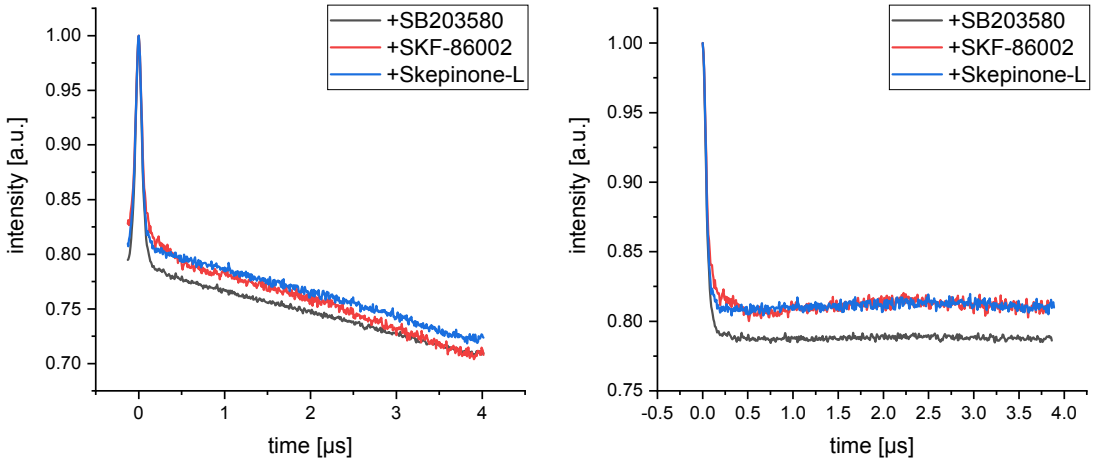

Figure S. 8: Inhibitor measurements with p38α 251. Left: Raw DEER data traces obtained for p38α 251 with the three type I inhibitors. Right: Form factors obtained for the DEER traces.

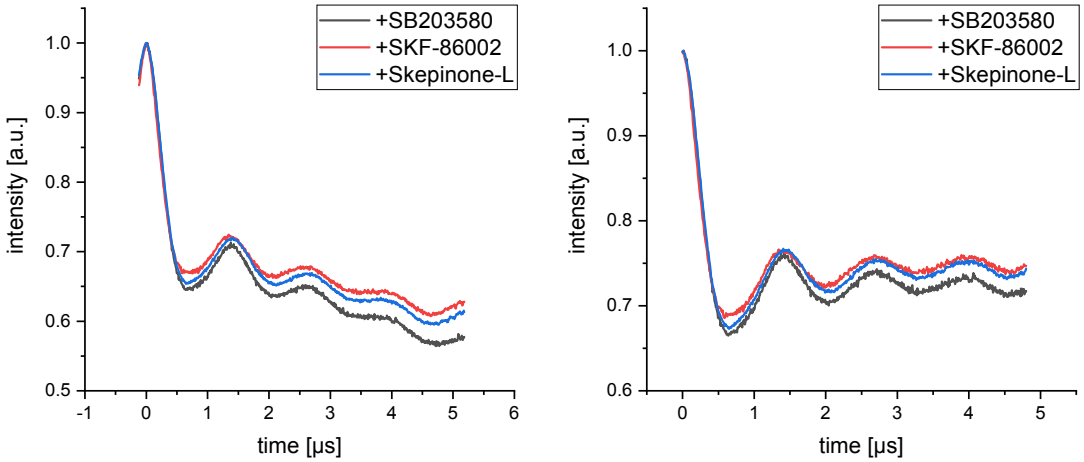

Figure S. 9: Inhibitor measurements with p38α 277. Left: Raw DEER data traces obtained for p38α 277 with the three type I inhibitors. Right: Form factors obtained for the DEER traces.

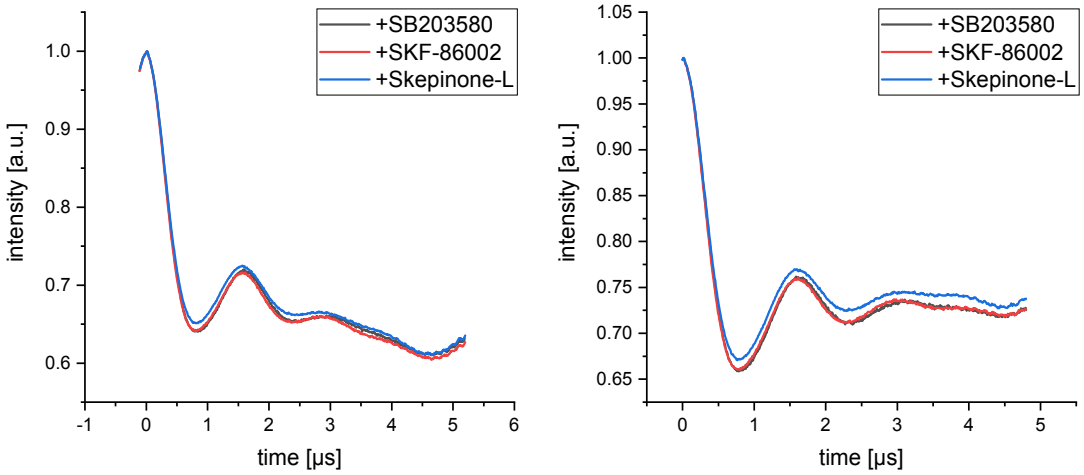

Figure S. 10: Inhibitor measurements with p38α 309. Left: Raw DEER data traces obtained for p38α 309 with the three type I inhibitors. Right: Form factors obtained for the DEER traces.

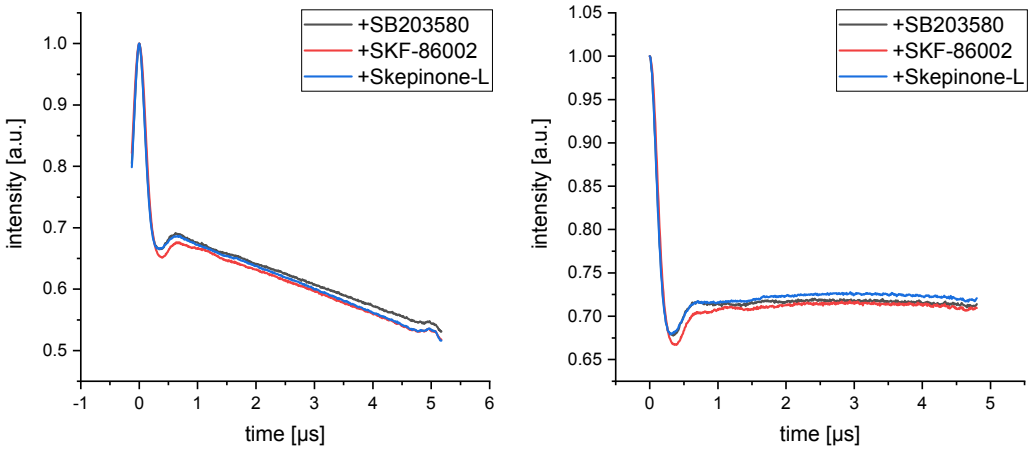

Figure S. 11: Inhibitor measurements with p38α 347. Left: Raw DEER data traces obtained for p38α 347 with the three type I inhibitors. Right: Form factors obtained for the DEER traces.

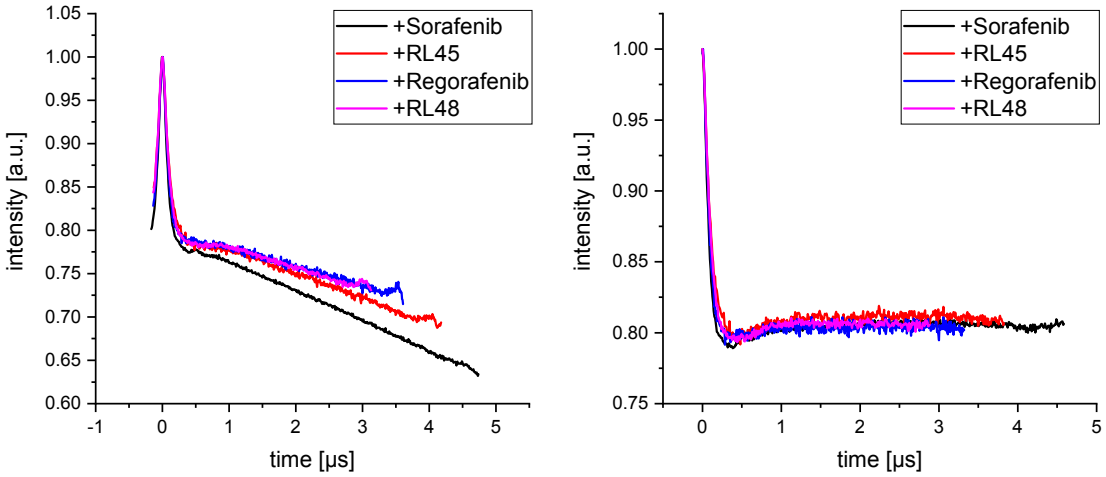

Figure S. 12: Inhibitor measurements with p38α 119. Left: Raw DEER data traces obtained for p38α 119 with the four type II inhibitors. Right: Form factors obtained for the DEER traces.

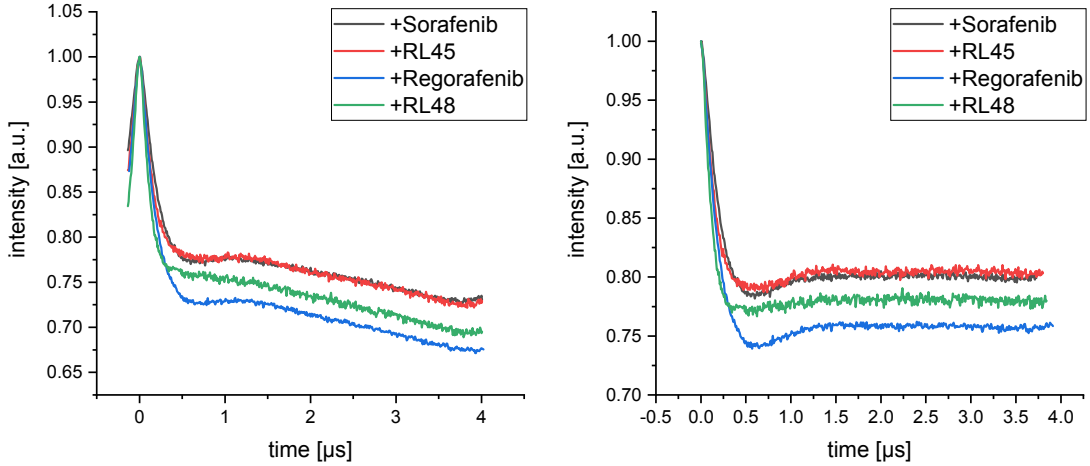

Figure S. 13: Inhibitor measurements with p38α 251. Left: Raw DEER data traces obtained for p38α 251 with the four type II inhibitors. Right: Form factors obtained for the DEER traces.

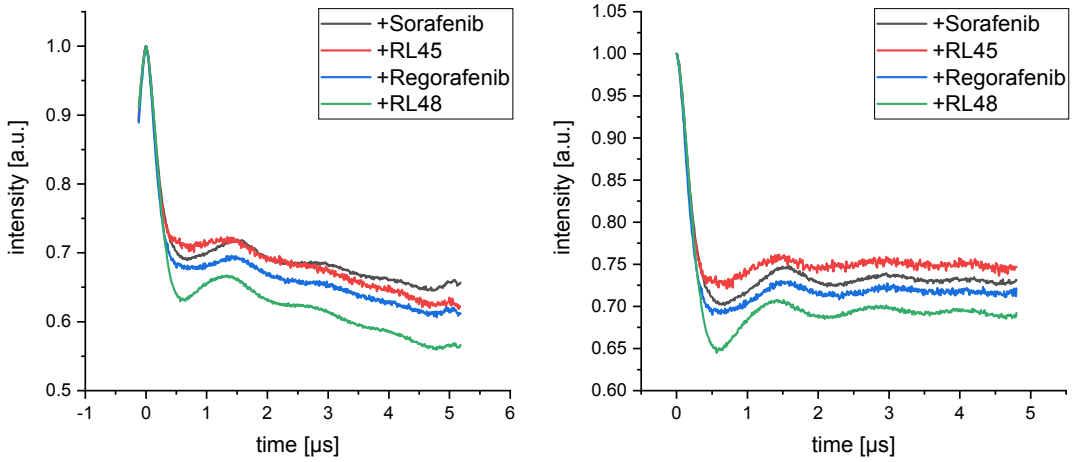

Figure S. 14: Inhibitor measurements with p38α 277. Left: Raw DEER data traces obtained for p38α 277 with the four type II inhibitors. Right: Form factors obtained for the DEER traces.

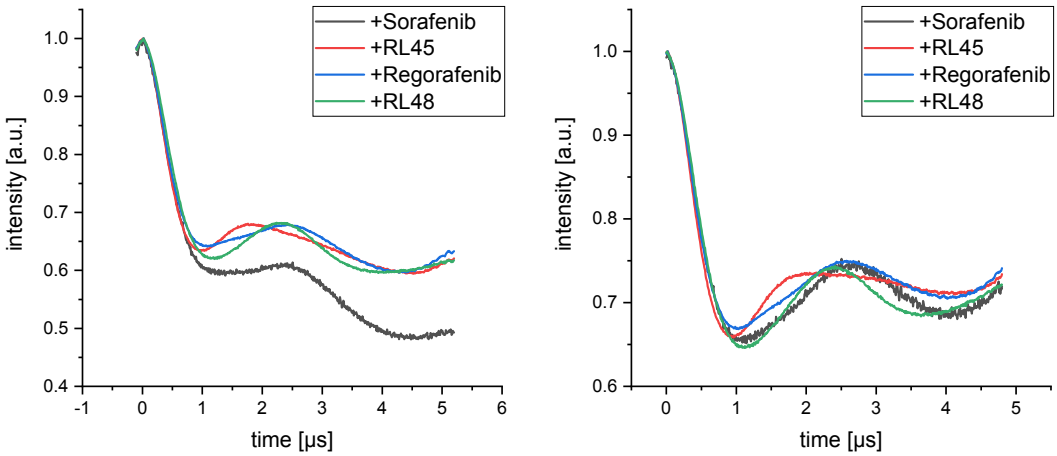

Figure S. 15: Inhibitor measurements with p38α 309. Left: Raw DEER data traces obtained for p38α 309 with the four type II inhibitors. Right: Form factors obtained for the DEER traces.

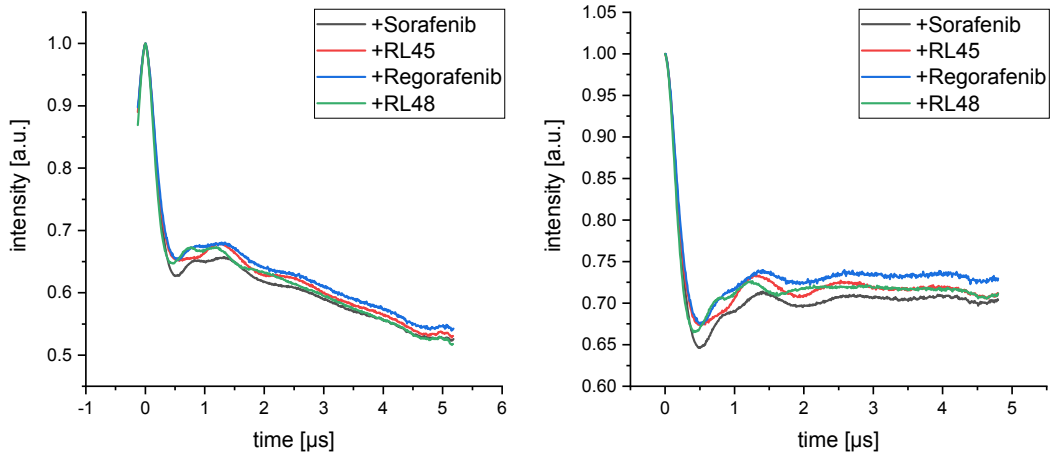

Figure S. 16: Inhibitor measurements with p38α 347. Left: Raw DEER data traces obtained for p38α 347 with the four type II inhibitors. Right: Form factors obtained for the DEER traces.

Simulated vs experimental distance distributions

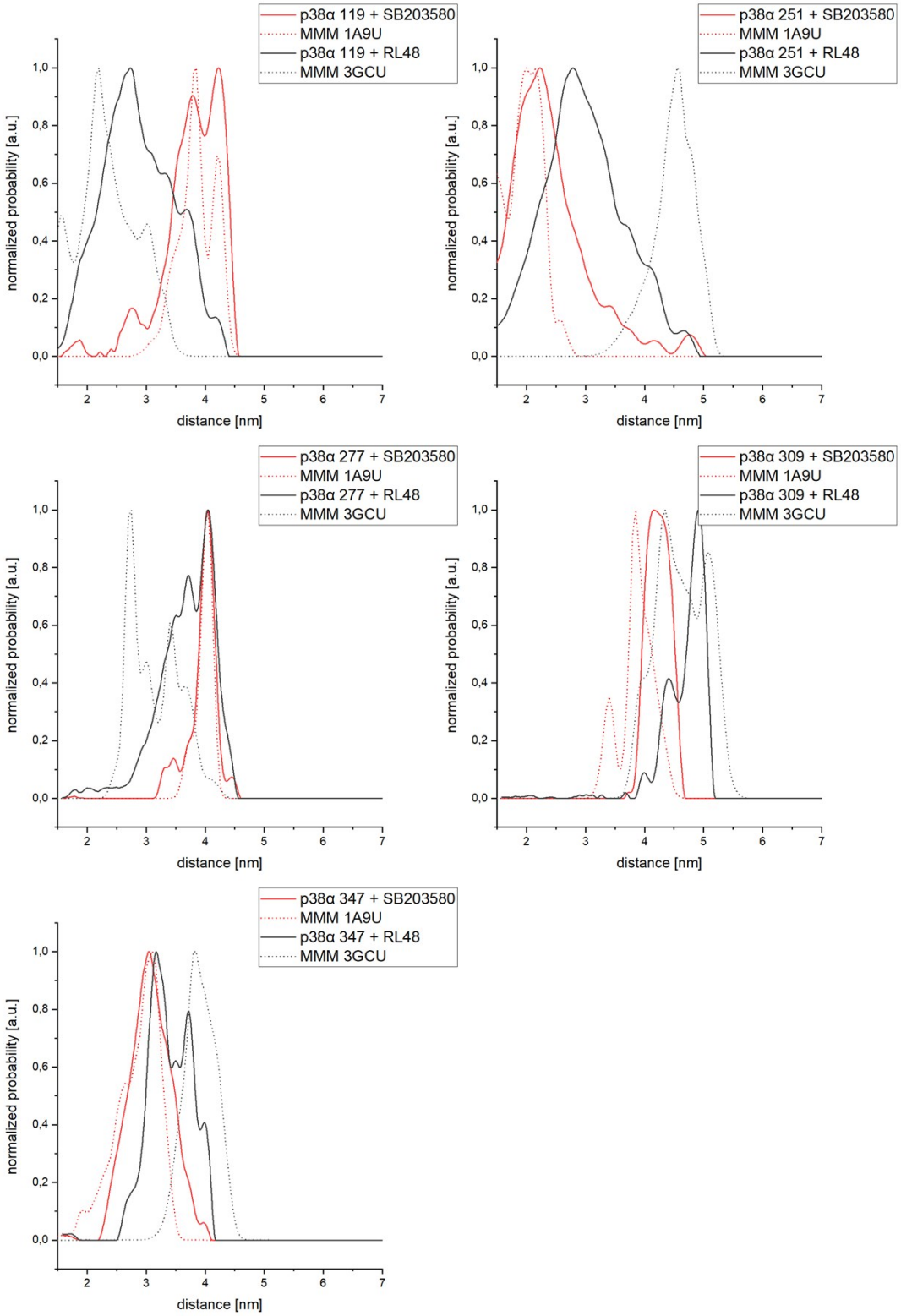

Figure S. 17: Comparison of simulated distance distributions (dotted lines) obtained via calculation of the spin label rotamer populations with experimental results (lines). Rotamer calculations were carried out using MMM[5] and the crystal structures 1A9U (p38α bound to SB203580) and 3GCU (p38α bound to RL48). As for experimental results, the experiments conducted in the presence of the inhibitors corresponding to the crystal structure environment are shown.

Distance distributions obtained for apo p38α and with type I inhibitors

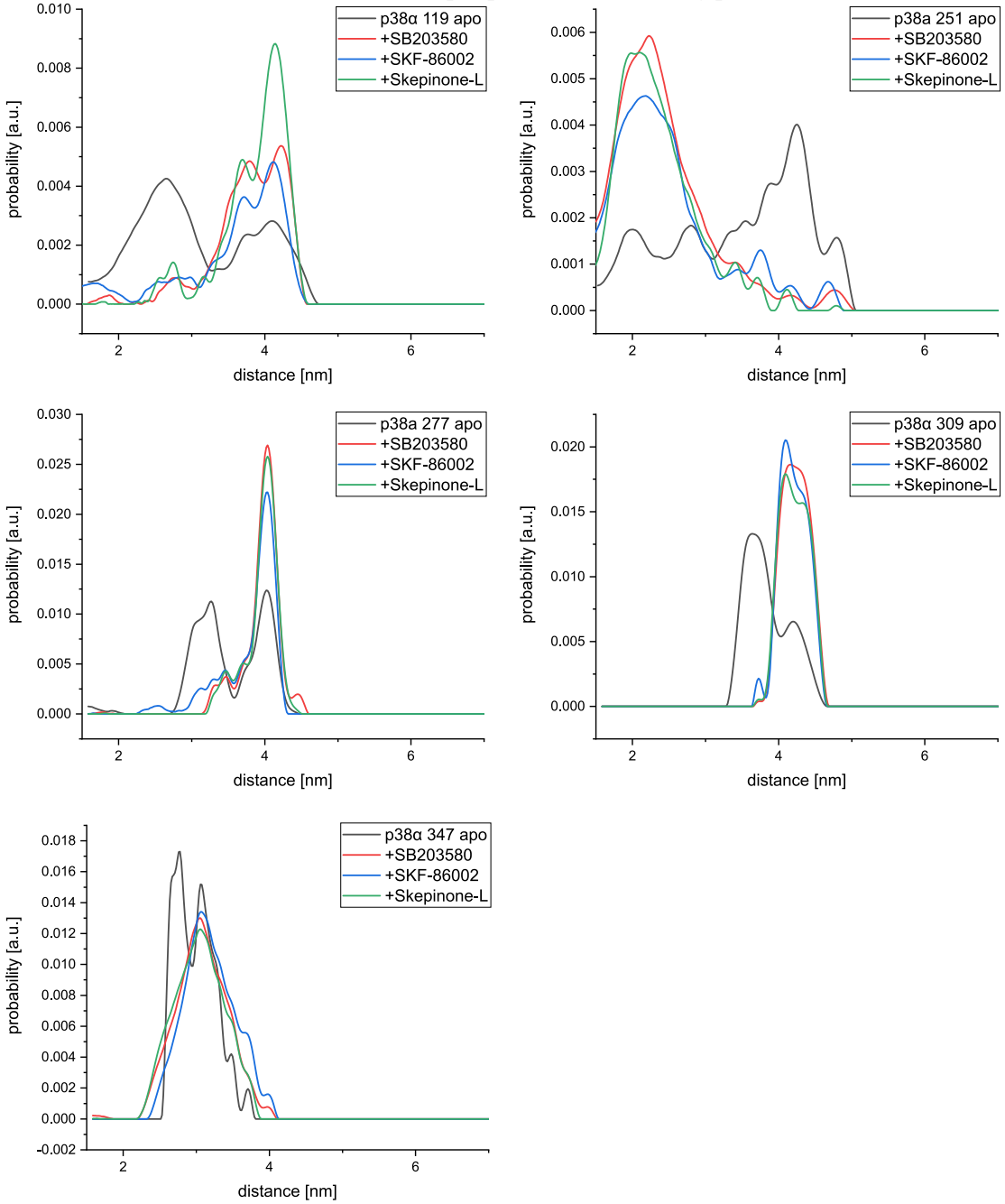

Figure S. 18: All distance distributions obtained for the five double mutants of p38α apo and in combination with the three type I inhibitors.

Distance distributions obtained for apo p38α and with type II inhibitors

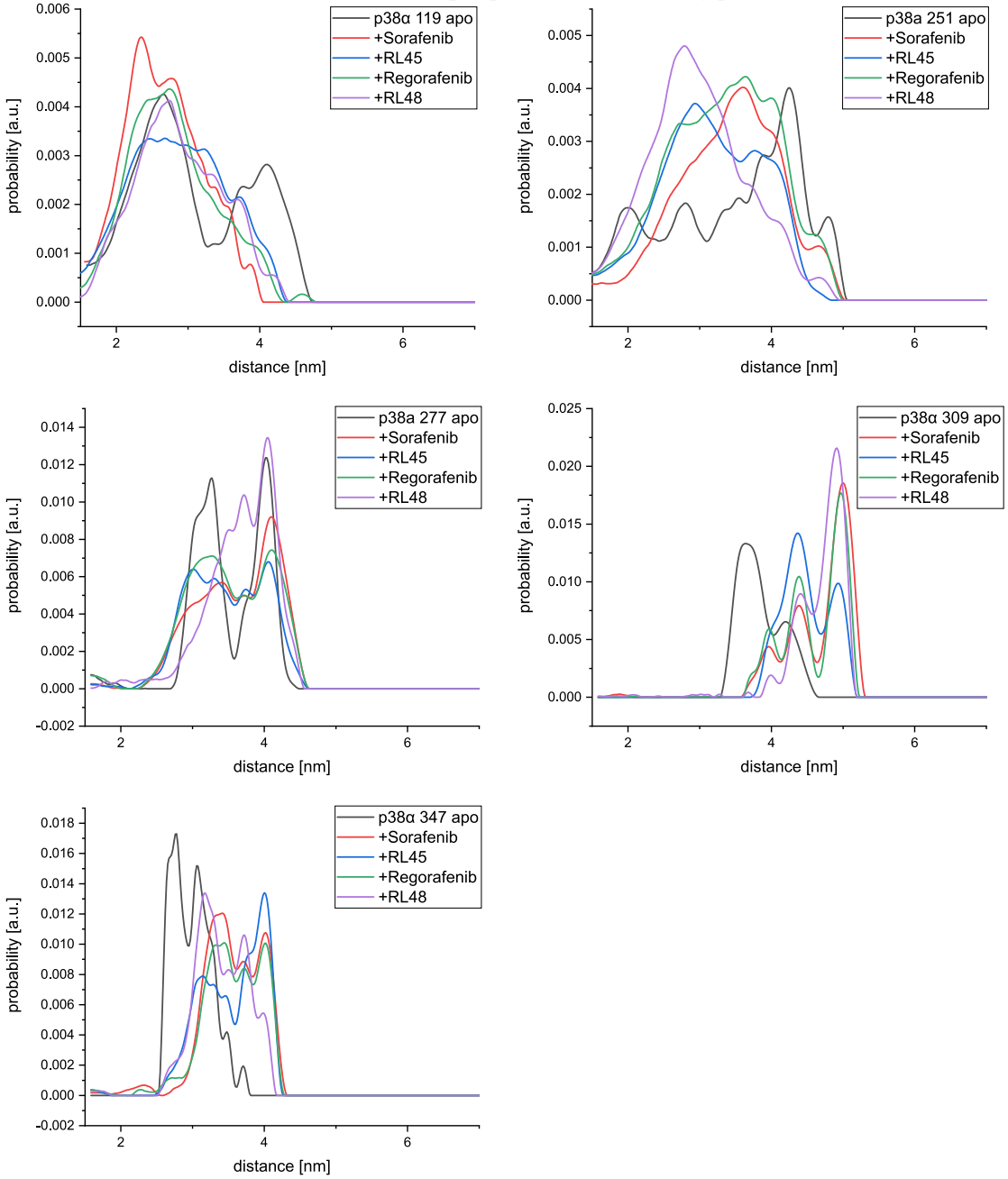

Figure S. 19: All distance distributions obtained for the five double mutants of p38α apo and in combination with the four type II inhibitors.

Multilateration comparison for type II inhibitors

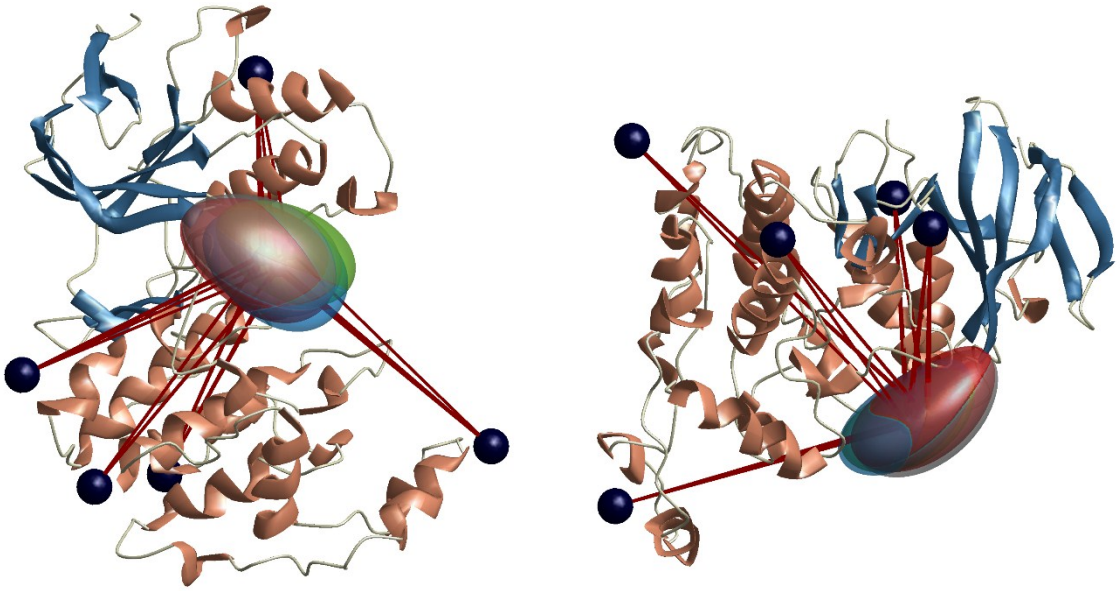

Figure S. 20: Multilateration for all type II inhibitors, structure 3GCU. The probability volumes for RL45 (blue), RL48 (green), Regorafenib (red) and Sorafenib (grey) are shown.

References

1. Simard, J. R.; Getlik, M.; Grütter, C.; Pawar, V.; Wulfert, S.; Rabiller, M.; Rauh, D., Development of a fluorescent-tagged kinase assay system for the detection and characterization of allosteric kinase inhibitors. *J Am Chem Soc* **2009**, *131* (37), 13286-13296.

2. Roser, P.; Weisner, J.; Simard, J. R.; Rauh, D.; Drescher, M., Direct monitoring of the conformational equilibria of the activation loop in the mitogen-activated protein kinase p38 alpha. *Chem Commun* **2018**, *54* (85), 12057-12060.

3. Pannier, M.; Veit, S.; Godt, A.; Jeschke, G.; Spiess, H. W., Dead-time free measurement of dipole–dipole interactions between electron spins. *J Magn Reson* **2011**, *213* (2), 316-325.

4. Jeschke, G.; Chechik, V.; Ionita, P.; Godt, A.; Zimmermann, H.; Banham, J.; Timmel, C.; Hilger, D.; Jung, H., DeerAnalysis2006—a comprehensive software package for analyzing pulsed ELDOR data. *Appl Magn Reson* **2006**, *30* (3-4), 473-498.

5. Jeschke, G., MMM: A toolbox for integrative structure modeling. *Protein Sci* **2018**, *27* (1), 76-85.

6. The PyMOL Molecular Graphics System, Version 2.1 Schrödinger, LLC.

7. Hagelueken, G.; Ward, R.; Naismith, J. H.; Schiemann, O., MtsslWizard: in silico spin-labeling and generation of distance distributions in PyMOL. *Appl Magn Reson* **2012**, *42* (3), 377-391.